Designing Scintillating Coordination Polymers Using a Dual-Ligand Synthetic Approach

Ana Arteaga[a], Alice Lulich[a], May Nyman[b], and Robert G. Surbella III[a]*

[a]Pacific Northwest National Laboratory, 902 Battelle Boulevard, Richland, WA 99354, United States.
[b]Department of Chemistry, Oregon State University, 153 Gilbert Hall, Corvallis, Oregon 97331, United States

***Email: robert.surbella@pnnl.gov**

Table of Content	**Page**

1. Synthetic Details

Reagents were purchased commercially from Sigma-Aldrich and used without further purification. The chemical reagents: DMF (anhydrous, 99.8%), 1,10-phenanthroline (phen, >98.0%), 2,2′:6′,2″-terpyridine (terpy, 99%,), 2,6-naphthalenedicarboxylic acid (2,6-ndc, >99%) or 1,4-naphthalenedicarboxylic acid (1,4-ndc, >99%), and $EuCl_3 \cdot 6H_2O$ (99.99% trace metals basis).

Synthesis:

$[Eu(terpy)(2,6\text{-}ndc)_{1.5}] \cdot H_2O$ (LP-1) was synthesized hydrothermally by combining 0.1 g of $EuCl_3 \cdot 6H_2O$ (0.27 mmol), 0.06 g of 2,6-ndc (0.27 mmol), 0.06 g of terpy (0.27 mmol) and 5 mL of ultrapure water (H_2O) into a 23 mL Teflon-lined acid digestion vessel. The reaction contents were heated to 110°C for 70 hours, and thereafter allowed to cool to room temperature. Clear, nearly colorless (faint green hue) rhombohedral-shaped crystals formed, Fig. S1. The crystals were washed three times with 5 mL of ethanol to remove excess ligand. Powder X-ray diffraction (PXRD) data collected on the bulk reaction product revealed an impurity that could not be identified, Fig. S5. The impurity is highlighted by the diffraction peak at 27° 2θ. The impurity was removed by washing the bulk reaction product with a mixture of ultrapure H_2O and 30% NH_4OH, followed by ethanol. The final yield of the reaction is 14.7%.

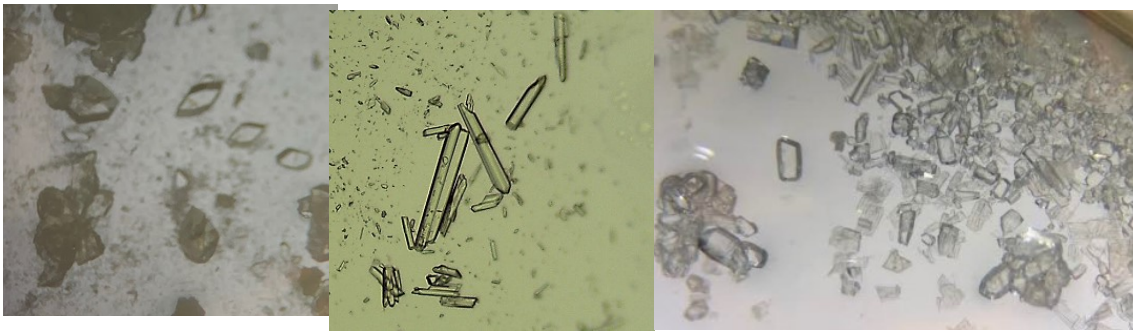

Fig. S1. Photo images of **LP-1** (left), **LP-2** (middle), and **LP-3** (right) crystals taken at x3 magnification.

[Eu(terpy)(1,4-ndc)(1,4-Hndc)] (LP-2) was synthesized hydrothermally by combining 0.1 g of $EuCl_3 \cdot 6H_2O$ (0.27 mmol), 0.08 g of 1,4-ndc (0.37 mmol), 0.09 g of terpy (0.38 mmol), and 2.5 mL of ultrapure H_2O in a 23 mL Teflon-lined acid digestion vessel. The reaction contents were heated to 110℃ for 70 hours, and thereafter allowed to cool to room temperature. Clear, nearly colorless, blade-like crystals with a faint green hue formed, Fig. S1. The crystals were washed three times with 5 mL of ethanol to remove any excess ligand. PXRD data collected on the bulk reaction product shows phase purity, Fig. S6. The final yield of the reaction is 37%.

[Eu(phen)(2,6-ndc)$_{1.5}$]·DMF (LP-3) was synthesized solvothermally by combining 0.1 g of $EuCl_3 \cdot 6H_2O$ (0.27 mmol), 0.06 g of 2,6-ndc (0.27 mmol), 0.1 g of phen (0.55 mmol) and 5 mL of DMF into a 23 mL Teflon-lined acid digestion vessel. The reaction contents were heated to 110 ℃ for 70 hours, and thereafter allowed to cool to room temperature. Clear, colorless blade-like and rhombohedral shaped crystals with a faint green color formed, Fig. S1. The crystals were washed three times with fresh DMF to remove any excess ligand. The crystals were unstable outside the mother liquor and prone to rapid degradation. Attempts to stabilize the material by solvent exchange with organic solvents (ethanol, acetone, isopropanol, etc.) were unsuccessful, and led to degradation.

2. Experimental and Relevant Data

Single Crystal X-ray Diffraction.

Reflection data of **LP-1** and **3** were collected using 0.5° ω and φ scans at 100(2) K on a Bruker D8 Venture diffractometer equipped with a Photon 100 CMOS detector and a Mo Kα source with a triumph monochromator (Table S1). The APEX III software suite1 was used to integrate the data and apply an absorption correction (SADABS).[1] Reflection data of **LP-2** were collected on a Rigaku Oxford Diffraction Synergy-S equipped with a PhotonJet-S Cu source (λ = 1.54178 Å) and HyPix-6000HE photon-counting detector. All the images were collected and processed using CrysAlisPro Version 40.21a, 40.53 and 40.81a (Rigaku Oxford Diffraction, 2018).[2] The reduced data were solved using direct methods via SHELXS3 and refined using SHELXL-153 within the

WINGX software suite.[3] Publication materials were prepared using EnCifer6[4] and all figures of the title compounds were generated using CrystalMaker® (V10.7.1): a crystal and molecular structures program for Mac and Windows. CrystalMaker Software Ltd, Oxford, England (www.crystalmaker.com).

All the nonhydrogen atoms in **LP-1**, **LP-2**, and **LP-3** were located on the difference Fourier maps and refined anisotropically. All H atoms associated with the carbon atoms were affixed to their parent atoms using a riding model. In **LP-1**, several of the C atoms of a 2,6-ndc ligand exhibit some signs of disorder (CheckCif Alert level B for Hirshfeld test) as well as some residual electron density surrounding the ring. This is caused by minor positional disorder of the ligand. We chose not to model this disorder as it was minor (no atoms were split or badly disordered). The lone solvent water molecule in **LP-1** was disordered over two positions and was modeled using Part Instructions. The H atoms associated with the water molecules in **LP-1** could not be modeled and refined with confidence (even after using heavy restraints) and were left unmodeled. In **LP-2**, the two η_1-1,4-ndc ligands are terminal and each feature one noncoordinated O atom of the carboxylate group. The carboxylate groups face one another and form head-on O-H···O hydrogen bonds with one another. The H atom site is likely partially occupied but is modeled only on one of the O atoms. This noncovalent interaction results in a short O-H···O bond distance (causing a CheckCif Alert B). We have ruled out common modeling errors and are confident in the connectivity and motif modeled. Specific to **LP-3**, we note several unresolved electron density peaks that trigger several CheckCif A, B, and C level alerts. Errors in unit cell and space group assignment were ruled out as was the possibility of twinning. These errors are therefore attributed to the large crystal size and heavy atoms located within the crystal structure.

Table S1. Selected crystallographic data for **LP-1**, **LP-2**, and **LP-3** at 100(2) K.

Compound	**LP-1**	**LP-2**	**LP-3**
Empirical Formula	$C_{33}H_{20}EuN_3O_7$	$C_{39}H_{24}EuN_3O_8$	$C_{33}H_{24}EuN_3O_7$
Formula mass	722.48	814.57	726.51
λ	Mo Kα 0.71073	Cu Kα 1.54184	Mo Kα 0.71073
Crystal Color and Habit	Light green to colorless, rhombohedral	Light green to colorless, blades	Light green to colorless, blades
Size	0.50 x 0.50 x 0.50	0.177 x 0.310 x 0.269	0.50 x 0.50 x 0.50
Crystal system	Triclinic	Monoclinic	Triclinic
Space Group	$P\bar{1}$	$P2_1/n$	$P\bar{1}$
a (Å)	8.9340(4)	9.75580(10)	11.2602(7)
b (Å)	11.4151(5)	18.23070(10)	12.0576(7)
c (Å)	13.6980(6)	18.76160(10)	12.2932(7)
α (°)	83.0660(10)°	90.0	78.341(3)
β (°)	81.1230(10)°	101.1880(10)	78.639(3)
γ (°)	83.4390(10)°	90.0	63.154(3)
Volume (Å^3)	1363.60(10)	3273.43(4)	1447.73(15)
D_{calc} (mg m^{-3})	1.760	1.653	1.667
Z	2	4	1
μ (mm^{-1})	2.358	14.233	2.222
No. of reflections measured	80387	100479	67463
No. of independent reflections	10487	6708	5976
R_{int}	0.0251	0.0623	0.0697
Final R_1 values ($I > 2\sigma(I)$)	0.0257	0.0299	0.0661
Final wR_2 (F^2) values ($I > 2\sigma(I)$)	0.0605	0.0779	0.1755
Goodness of fit on F^2	1.097	1.066	1.150
CCDC number	2255873	2255874	2255875

Secondary building unit (SBU) analysis: The analysis was performed with topcryst.com.[5] The RCSR three-letter codes[6] were used to designate the network topologies. The TTD collection[7] was used to determine the topological type of the crystal structure.

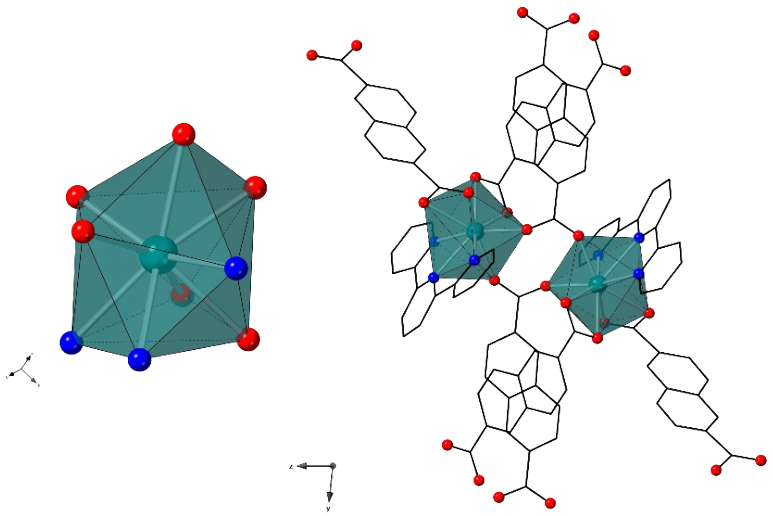

Fig. S2. (left) **LP-1** features nine-coordinate metal centers that have a tricapped trigonal prismatic geometry. (right) Each metal center is coordinated by one terpy and four total 2,6-ndc ligands. Two 2,6-ndc ligands bridge the neighboring metal centers together, forming pseudo-dimeric units.

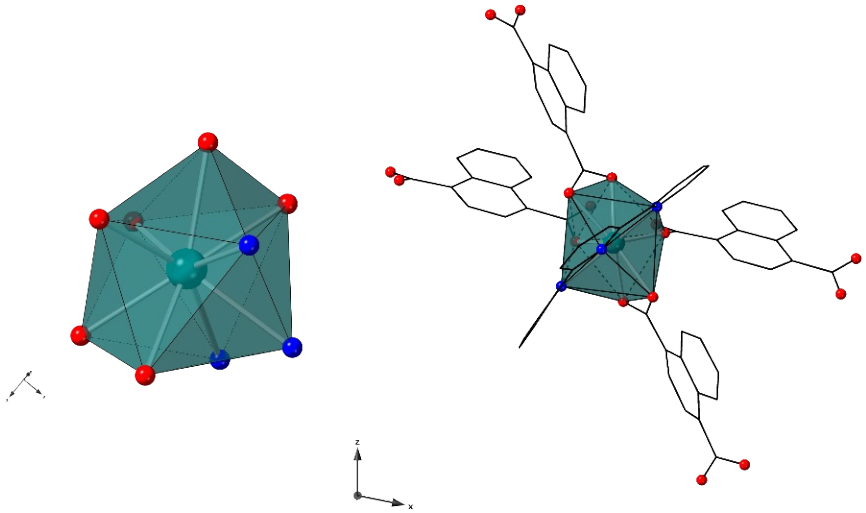

Fig. S3. (left) **LP-2** has a nine-coordinate metal centers that feature a tricapped trigonal prismatic geometry. (right) The Eu^{3+} metal centers are coordinated by one terpy and four total 1,4-ndc ligands.

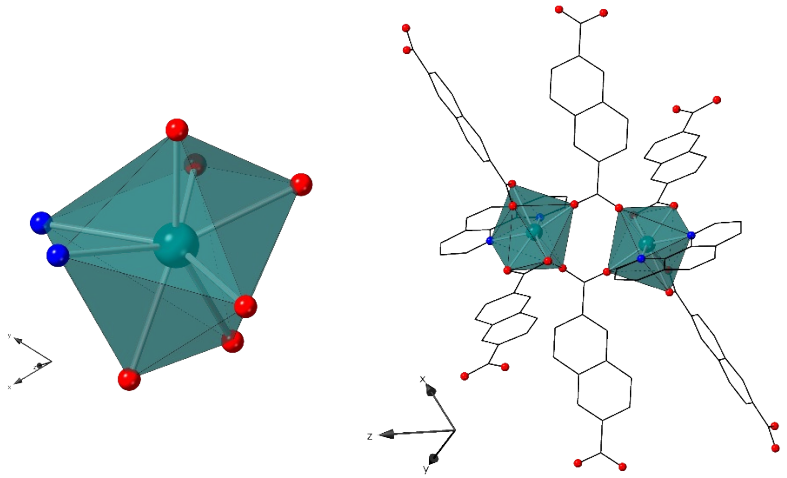

Fig. S4. (left) **LP-3** contains eight-coordinate metal centers that feature a dodecahedral (bisdisphenoid) geometry. (right) Each metal center is coordinated by one phen and four 2,6-ndc ligands. The metal centers form dimeric nodes through linkages created by the 2,6-ndc ligands.

Surface Area Analysis. Nitrogen adsorption isotherms were collected for **LP-1** and **LP-2** on 11.7 mg sized powder samples. The samples were activated prior to measurement by heating to 100°C under vacuum for 12 hours. Data were collected using a BET Quantachrome Autosorb iQ3 unit at 77 K. Outgassing theory was used to derive the surface area values and single point adsorption at P/P0 ≈ 0.99.

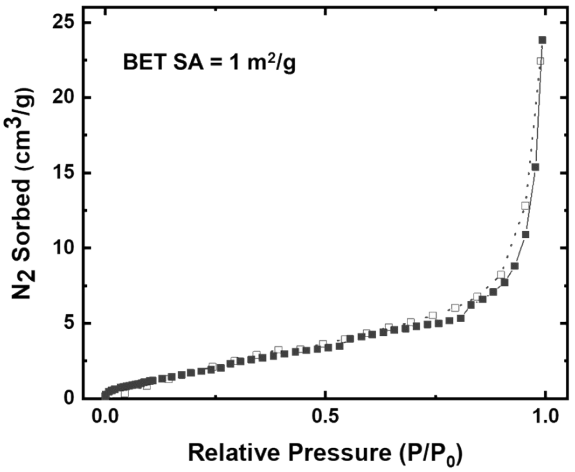

Fig. S5. N_2 adsorption (filled) and desorption (unfilled) isotherms of **LP-1** at 77 K with calculated BET surface areas.

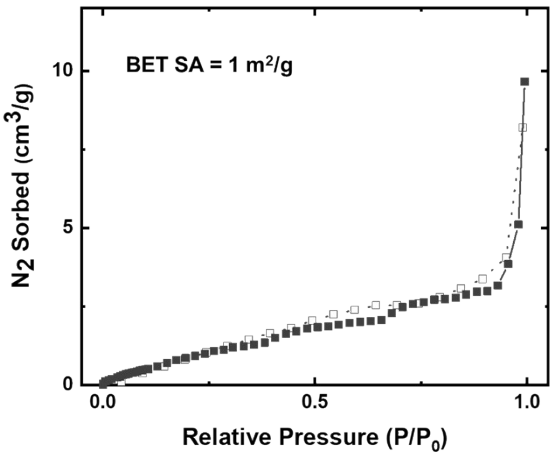

Fig. S6. N_2 adsorption (filled) and desorption (unfilled) isotherms of **LP-2** at 77 K with calculated BET surface areas.

Thermogravimetric Analysis. Compounds **LP-1** and **LP-2** were analyzed using a SDT Q600 V20.9 Build 20 TGA-DSC. Roughly 10 mg of each powdered sample were heated from 25°C to 700°C at a heating rate of 10°C min^{-1} using either $Ar_{(g)}$ or air (21% $O_{2(g)}$) as the carrier gases.

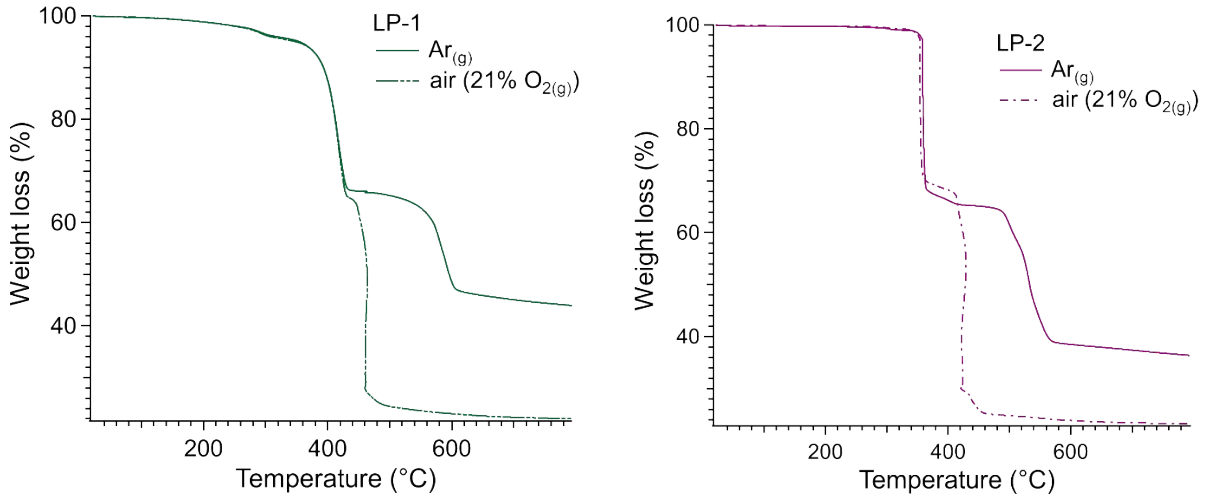

Fig. S7. The thermogravimetric analysis data of **LP-1** (left) and **LP-2** (right) in $Ar_{(g)}$ and in air.

Powder X-ray Diffraction. Data on **LP-1** and **LP-2** were collected using a Rigaku Ultima IV diffractometer equipped with a Cu sealed tube X-ray source (1.6 kW). The scans were collected in 0.02° count binning steps with a 1°/minute scan rate. The instrument featured a 10 mm divergence slit, 0.5 mm incident slit, 5° primary and receiving side solar slits, and a Ni foil filter to reduce contributions from Kβ.

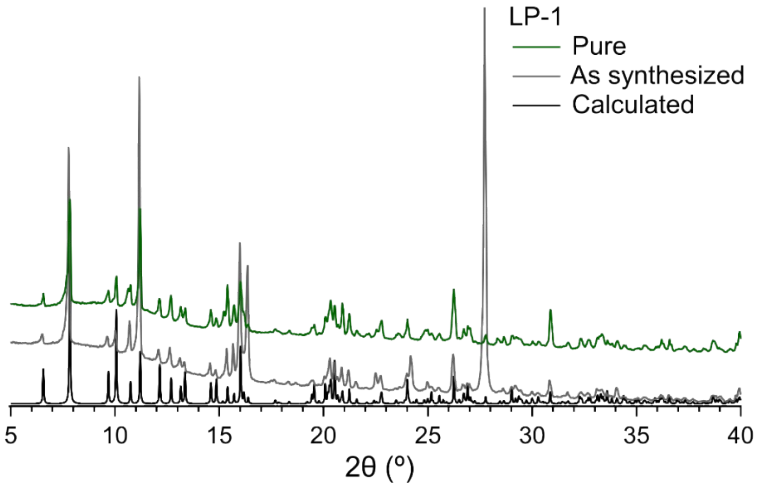

Fig. S8. The experimental and calculated diffractogram of **LP-1** before and after removing the impurity observed at 27° 2θ.

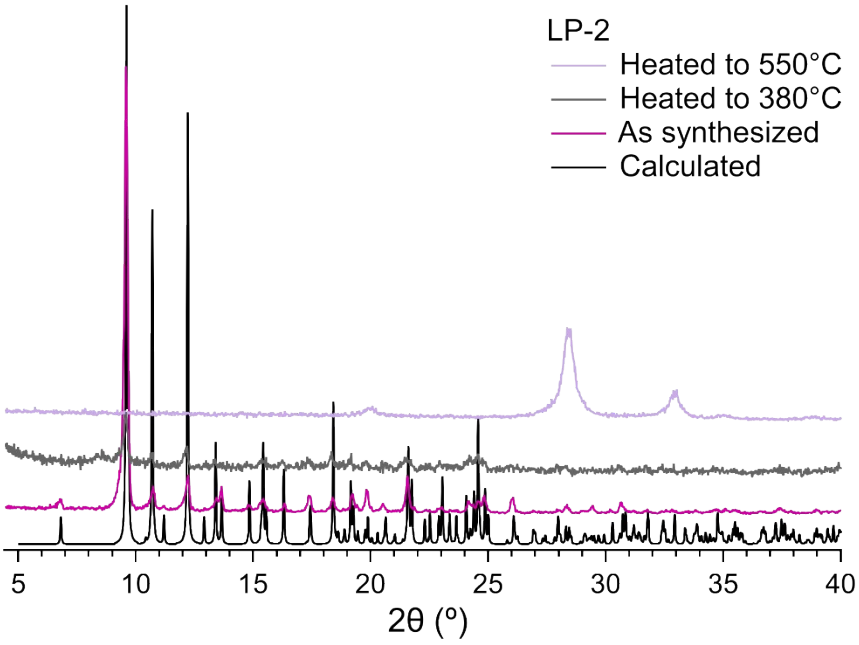

Fig. S9. The experimental and calculated diffractogram of **LP-2** showing the loss of crystallinity and the degradation to Eu_2O_3 after heat treatment of 380°C and 550°C, respectively.

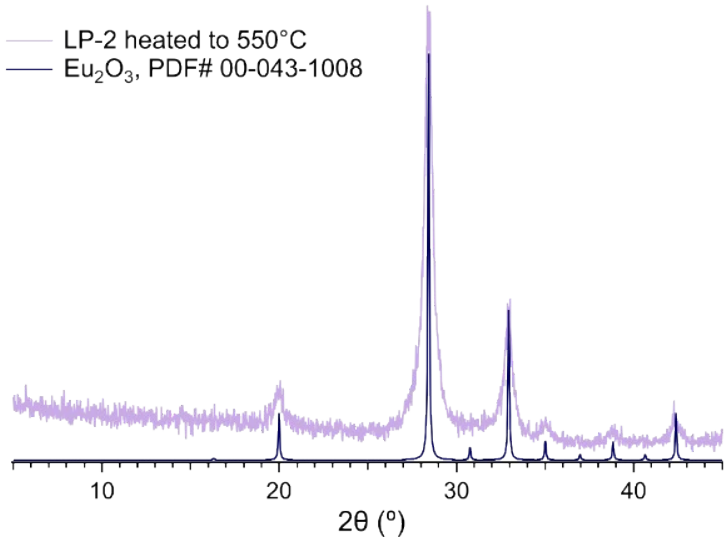

Fig. S10. The experimental diffractogram of **LP-2** after heat treatment at 550°C and Eu_2O_3, ICDD PDF number 00-043-1008.

Diffuse Reflectance. Solid-state DR data were collected on bulk material of **LP-1** and **LP-2** using a Cary-5000 UV-vis-NIR spectrometer with a DRA-2500 external DR accessory.

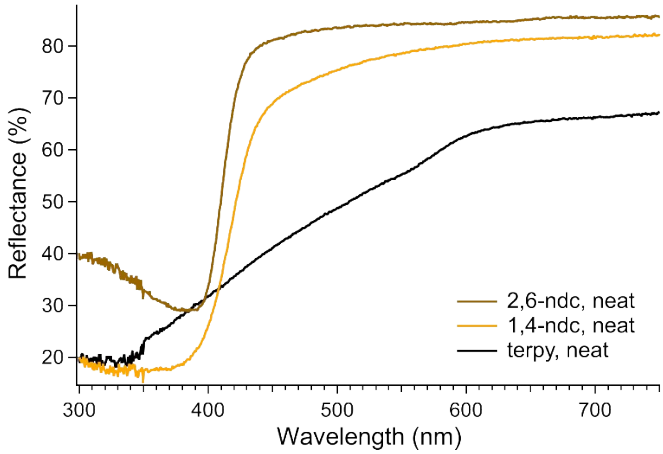

Fig. S11. DR spectra of 2,6-ndc, 1,4-ndc and terpy ligands.

Photoluminescence Characterization. Luminescence data of powdered samples of **LP-1** and **LP-2**, and single crystals of **LP-3** immersed in DMF were used for data collection. The samples were loaded into quartz NMR tubes and measurements were taken within a quartz dewar at 298 K using a Horiba Nano-log®-3 PL spectrophotometer outfitted with a 450W Xe excitation source. The data were collected at 90° from the excitation source and recorded using a UV-Visible PMT detector (185-850 nm). All data were processed using the FluorEssence software (V.3.9.0.1) and Origin (V.8.6001).

Table S2. The excitation and emission spectra transition assignments.

Excitation spectra				Emission spectra			
LP-1 λ (nm)	**LP-2 λ (nm)**	**LP-3 λ (nm)**	**Assignment**	**LP-1 λ (nm)**	**LP-2 λ (nm)**	**LP-3 λ (nm)**	**Assignment**
322-379	324-399	325-377	ligand	579	-	580	$^5D_0 \rightarrow {}^7F_0$
395		395	$^5L_6 \leftarrow {}^7F_0$	590	588, 594	592	$^5D_0 \rightarrow {}^7F_1$
416		416	$^5D_3 \leftarrow {}^7F_0$	619	617	616	$^5D_0 \rightarrow {}^7F_2$
466	466	466	$^5D_2 \leftarrow {}^7F_0$	649	649	651	$^5D_0 \rightarrow {}^7F_3$
526	526	526	$^5D_1 \leftarrow {}^7F_0$	695	690	697	$^5D_0 \rightarrow {}^7F_4$
535	535	535	$^5D_6 \leftarrow {}^7F_1$				

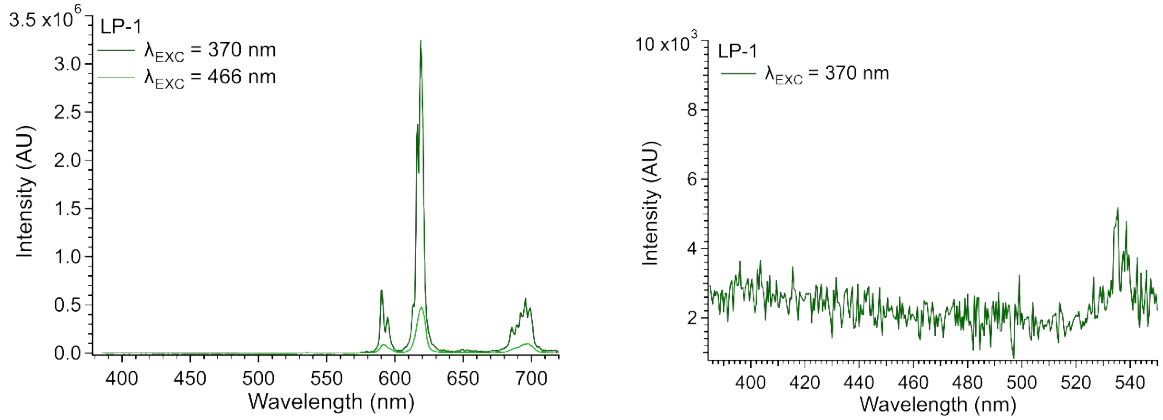

Fig. S12. The emission spectra of **LP-1** collected at 298 K.

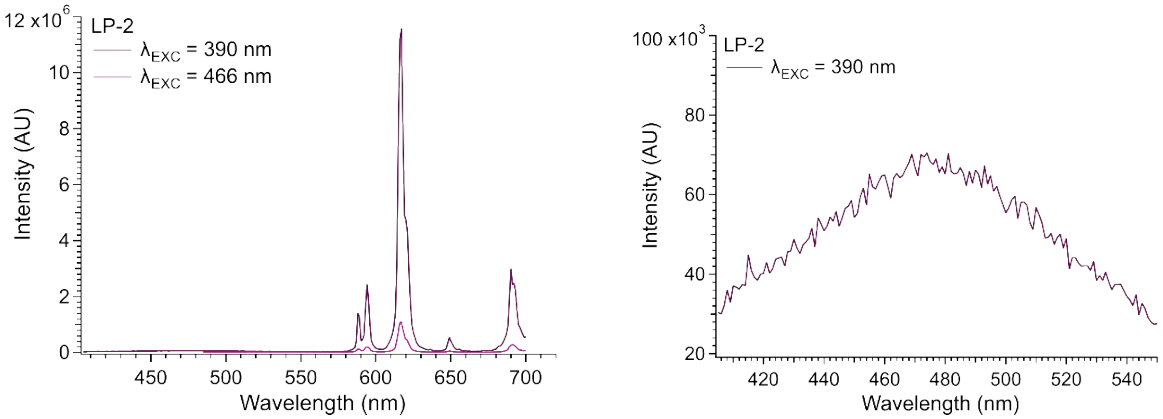

Fig. S13. The emission spectra of **LP-2** collected at 298 K.

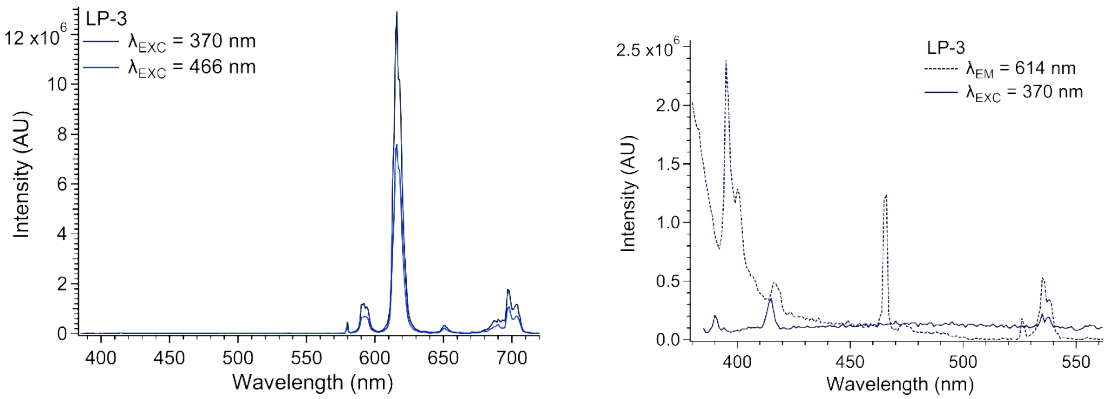

Fig. S14. The emission spectra of **LP-3** collected at 298 K.

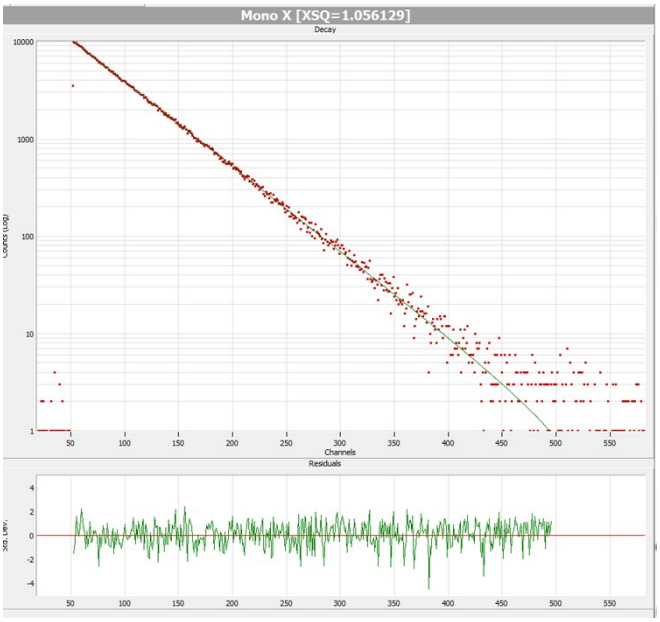

Fig. S15. Luminescence decay curves, curve fitting, and the χ^2 of LP-1 collect at 298 K.

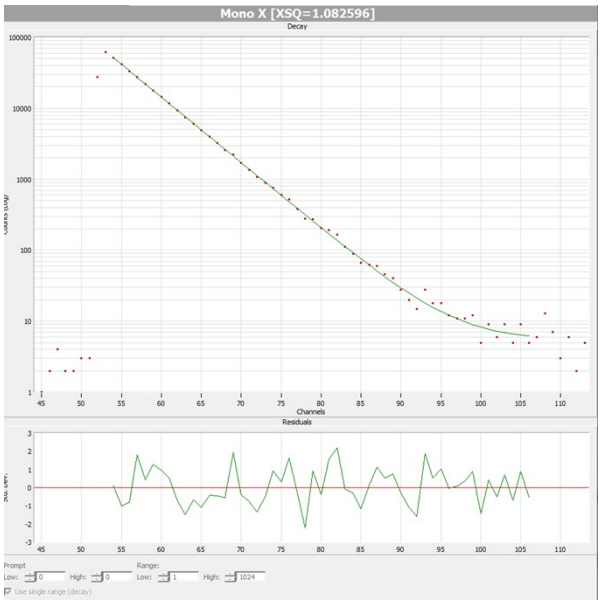

Fig. S16. Luminescence decay curves, curve fitting, and the χ^2 of LP-2 collect at 298 K.

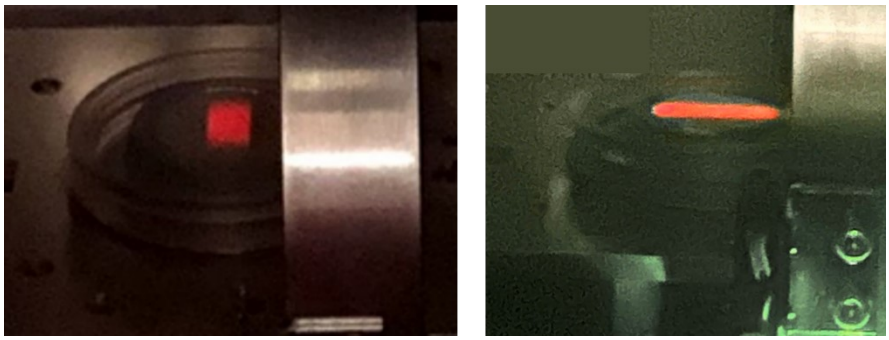

Fig S17. Compound **LP-1** (left) and **LP-2** (right) produce bright red emission when exposed to soft X-rays (Cu Kα, 8.04 keV).

Attenuated Total Reflectance Fourier Transform Infrared spectroscopy (ATR-FTIR) was performed on samples of **LP-1** and **LP-2**. The data were collected using a Bruker Lumos – FTIR spectrometer outfitted with an attenuated total reflection accessory and analyzed using the OPUS software (V.7.2).

Compound **LP-1** and **LP-2** display a series of vibrational bands between 1600–630 nm that correspond to stretching modes of C–C, C–O, C–H, and C–N bonds present in the organic ligands.[8-15] Between 3400–3600 nm the O–H stretch of the lattice and surface water molecules are observed.[16]

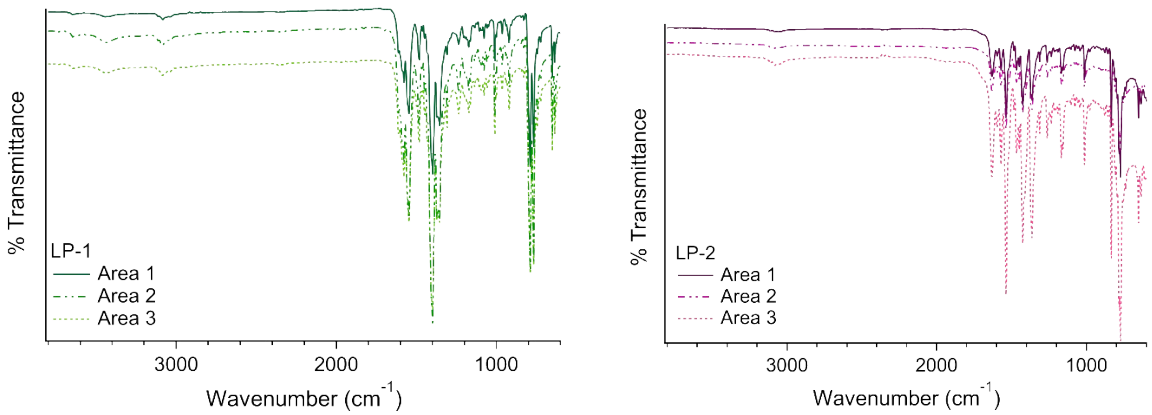

Fig. S18. Bulk crystalline material of **LP-1** (left) and **LP-2** (right) were each analyzed via FTIR in three areas to demonstrate homogeneity.

Table S3. Summary of **LP-1** vibrational bands and assignments.

Peak Energy (cm^{-1})	**Stretches**
3633	$\nu(H_2O)$
3435	$\nu(H_2O)$
3114	$\nu(H_2O)$
3086	ν_{sym}(C—H)
3033	ν_{sym}(C—H)
3007	$\nu(H_2O)$
1611	ν(C=O)
1589	ν (C=C)
1597	ν (C=C)
1546	ν (COO)
1483	ν (C=C), ν (C—H)
1470	ν (C=C), ν (C—H)
1454	ν (C=C)
1429	ν (COO)
1397	ν (C=C), ν (C—H)
1369	ν (C=O)
1309	ν (C=C), ν (C—H), ν(C=O)
1234	ν(C=O), ν (C—N)
1170	vib. of C3-C4 bond
1161	ν (C—H)
1136	ν (C—H)
1076	CH-wagg.
960	C=C bending, disubstituted
919	δ(C—H)
828	δ(C—H)
856	CH-wagg.
834	CH-wagg
807	CCC bend; ring def.
790	Napthalene ring
759	CH wagg (+) (036)
731	δ(C—H)
655	ν (C—H)
633	CCC bend, in two rings (-); CC-t

Table S4. Summary of **LP-2** vibrational bands and assignments.

Peak Energy (cm^{-1})	**Stretch**
3111	$\nu(H_2O)$
3081	ν_{sym}(C—H)
1631	ν(C=O)
1597	ν (C=C), ν (C=N)
1570	ν (C=N)
1536	ν (C=C)
1483	ν (C=C), ν (C—H)
1466	ν (C=C), ν (C—H)
1448	ν (C=C)
1425	ν_{sym}(OCO)
1363	ν (C=C), ν (C—H)
1311	ν (C—N)
1262	ν_{asym}(COO), ν (C—N)
1234	ν (C—N)
1213	ν (C—H)
1189	ν (C—H)
1167	ν (C—H)
1157	ν (C=C), ν (C—H)
1077	ν_{asym}(COO
1057	δ (C—H)
1041	ν (C=C)
1012	CH-wagg.
917	CH-wagg.
876	δ (C—H)
833	CH-wagg.
794	CH-wagg.
784	CH-wagg.
774	Breathing
651	CH

3. References

1. G. M. Sheldrick, *SADABS, Siemens Area Detector Absorption Correction Program, University of Göttingen: Göttingen, Germany*, 2008.
2. *CrysAlisPRO, Agilent, Agilent Technologies Ltd* 2014.
3. L. Farrugia, *J. Appl. Crystallogr.*, 2012, **45**, 849-854.
4. F. H. Allen, O. Johnson, G. P. Shields, B. R. Smith and M. Towler, *J. Appl. Cryst.*, 2004, **37**, 335-338.
5. V. A. Blatov, A. P. Shevchenko and D. M. Proserpio, *Cryst. Growth Des.*, 2014, **14**, 3576-3586.
6. M. O'Keeffe, M. A. Peskov, S. J. Ramsden and O. M. Yaghi, *Acc. Chem. Res.*, 2008, **41**, 1782-1789.
7. E. V. Alexandrov, A. P. Shevchenko and V. A. Blatov, *Cryst. Growth Des.*, 2019, **19**, 2604-2614.
8. Z. Demircioğlu, A. E. Yeşil, M. Altun, T. Bal-Demirci and N. Özdemir, *J. Mol. Struct.*, 2018, **1162**, 96-108.
9. Infrared Spectroscopy Absorption Table, https://chem.libretexts.org/Ancillary_Materials/Reference/Reference_Tables/Spectroscopic_Reference_Tables/Infrared_Spectroscopy_Absorption_Table).
10. Z. Wang, C.-M. Jin, T. Shao, Y.-Z. Li, K.-L. Zhang, H.-T. Zhang and X.-Z. You, *Inorg. Chem. Commun.*, 2002, **5**, 642-648.
11. R. Łyszczek, Z. Rzączyńska, A. Kula and A. Gładysz-Płaska, *JAAP*, 2011, **92**, 347-354.
12. J.-C. Wu, C.-W. Jin, D.-H. Zhang, N. Ren and J.-J. Zhang, *Thermochim. Acta*, 2015, **620**, 28-35.
13. R. Łyszczek and A. Lipke, *Microporous and Mesoporous Mater*, 2013, **168**, 81-91.
14. V. V. Butova, O. A. Burachevskaya, I. V. Ozhogin, G. S. Borodkin, A. G. Starikov, S. Bordiga, A. Damin, K. P. Lillerud and A. V. Soldatov, *Microporous and Mesoporous Mater*, 2020, **305**, 110324.
15. I.-H. Choi, Y. Kim, D. N. Lee and S. Huh, *Polyhedron*, 2016, **105**, 96-103.
16. F. Cheng, Q. Cao, Y. Guan, H. Cheng, X. Wang and J. D. Miller, *Int. J. Miner. Process.*, 2013, **122**, 36-42.